Assessing the potential of the recycled plastic slow pyrolysis for the production of streams attractive for refineries

Roberto Palos[a,b], Alazne Gutiérrez[a,]*, Francisco J. Vela[a], Jon A. Maña[a], Idoia Hita[a], Asier Asueta[c], Sixto Arnaiz[c], José M. Arandes[a] and Javier Bilbao[a]

[a] *Department of Chemical Engineering, University of the Basque Country UPV/EHU, PO Box 644, 48080 Bilbao, Spain*

[b] *Department of Chemical and Environmental Engineering, University of the Basque Country UPV/EHU, Plaza Europa 1, 20018 Donostia-San Sebastian, Spain*

[c] *Gaiker Technological Center, Parque Tecnológico, Edificio 202, 48170 Zamudio, Spain*

(*) corresponding author: alazne.gutierrez@ehu.eus

ABSTRACT

The slow pyrolysis of recycled high-density polyethylene (HDPE) has been investigated in a batch autoclave reactor at 430–490 °C and reaction times of 15–60 min, with the aim of obtaining the maximum yield of plastic oil (PO) with an adequate composition for its subsequent valorization in refinery. Specifically, PO yields up to 85-90 wt% have been achieved operating at 430 °C and 15-37.5 min, noting that the obtained yields strongly depend on temperature and, to a lesser extent, on reaction time. Simulated distillation and gas chromatography analyses of PO have shown its potential for its valorization in a waste refinery scheme targeting the production of alternative fuels. Thus, the PO obtained at 430 °C and 15 min is suitable to be co-fed to the fluidized catalytic cracking (FCC) unit

since it has a simulated distillation curve similar to that of vacuum gasoil (VGO). On the other hand, the PO obtained at 430 °C at the longest reaction time and those obtained at 460 °C are suitable to be fed together with light cycle oil (LCO) into a hydroprocessing unit. The composition of naphtha and middle distillates of PO reveals that these fractions are appropriate for their blending with commercial diesel and gasoline pools after a mild hydrotreating to reduce their olefin content.

Keywords: Plastic waste; Recycled HDPE; Slow pyrolysis; Liquid oil; Waste-refinery; Fuel

1. Introduction

The global production of plastics has been steadily increasing, up to 348 Mt in 2017, with an annual growth of ca. 1.5 % [1]. After reaching its end of life, a great fraction of these plastics ends up in municipal solid waste (MSW), where they constitute around 7 wt%, causing serious environmental hurdles due to their low biodegradability and the lack of large-scale recycling solutions [2]. Nonetheless, there is a worldwide pressing need for plastic recycling in order to avoid their uncontrolled landfilling, where plastics are degraded forming microplastics (particle size < 5 mm), which have an upsetting ecological impact on the soil [3] and on marine [4] and freshwater ecosystems [5].

Primary and secondary (mechanical) recycling routes offer good perspectives for their implementation at small and medium scale [6]. However, the large amount of formed waste plastics formed advices for ternary recycling routes for the large-scale production of fuels and chemicals, as well as the recovery of the monomers [7,8]. Among the thermochemical processes for plastic valorization, pyrolysis attracts great attention [9,10], since it allows for obtaining high oil yields from addition polymers, such as polyolefins, and for tailoring the composition of the oil to be used as a fuel. Furthermore, Fivga and Dimitrou [11] have proven that pyrolysis is economically viable at a large scale. Even though gasification has also acquired a remarkable technological development [12], the reaction technologies for the production of fuels and commodities from syngas require of important capital investments. Amongst the different pyrolysis alternatives, fast pyrolysis (at low temperatures with high heating rates and short residence time of the volatiles) can be performed in continuous regime with different types of reactors, e.g. fluidized bed, spouted bed, ablative [7,10,13]. The use of an in-situ located catalyst is a promising option to control the composition of gaseous and liquid products [14–17].

Moreover, the catalyst can be located ex-situ to intensify the recovery of monomers and adjust the composition of the liquid product [18,19].

On the basis of the socio-economic factors that determine the installation of waste plastics recycling units, a strong tendency is to associate the recycling of plastics, which are obtained from crude oil processing derivates, with the petrochemical industry. For this purpose, already depreciated refinery units would be used (waste refinery), i.e. fluidized catalytic cracking (FCC) and hydroprocessing units, because of their high capacity and versatility. Thereby, waste plastics could be integrated into different stages of the manufacturing chain of fuels and commodities, which could be marketed together with those derived from the usual oil streams with their composition fitted to legal requirements. The integration of the valorization of plastics into refinery streams has been addressed in the literature with different strategies. Among them, one can find the co-cracking of plastics and different refinery streams, such as light cycle oil (LCO), a highly aromatic stream from FCC units, and vacuum gasoil (VGO), the current feedstock to FCC unit which comes from the vacuum distillation unit [20–24], and the hydroprocessing of plastics blended with LCO [25] or vacuum residue (VR) [26,27]. The main physicochemical properties of standard VGO and LCO are collected in Table S1.

For the integration of pyrolysis with other refinery processes, the slow pyrolysis (long isothermal holding time) of plastics could be performed at small and moderate scale, in delocalized units, obtaining a high yield of plastic oil (PO) [28–30]. The pyrolysis unit, of simple design, would be installed at the MSW plastic collection and segregation point and the PO obtained would be afterwards transported to a refinery for its large-scale processing. In addition, with the valorization of the PO, the refinery would fulfill the social function of plastics recycling. It should also be taken into account that, given the

high capacity of the FCC and hydroprocessing units, the co-feeding of PO in a small ratio together with the current feedstock would be enough for the complete recovery of the plastics collected in a wide geographic environment.

This work mainly focuses on the interest of the PO from HDPE pyrolysis as a potential feedstock for refineries and so, its valorization in a refinery unit (FCC or hydroprocessing units) where, depending on its composition, it would be co-fed with Vacuum Gas Oil (VGO) or Light Cycle Oil (LCO). Based on all the premises, this work delves into the effect of temperature and reaction time on the quality and composition of the PO obtained from the slow pyrolysis of HDPE. The runs have been performed in a batch reactor pursuing the production of a high-quality liquid product suitable to be considered as a source of fuels and/or commodities. Insight into product composition and quality has been gathered by means of simulated distillation and gas chromatography analyses for evaluating the properties and composition of the PO to assess its interest to be co-fed to a refinery unit, as well as the interest of its naphtha and middle distillates fractions as components of the commercial gasoline and diesel pools, respectively.

2. Experimental

2.1. Characterization of the plastic feed

The plastic feed consists on recycled HDPE pellets (obtained after sorting, washing and shredding of HDPE waste) supplied by Gaiker Technological Centre (Zamudio, Spain). The main physicochemical properties of the recycled HDPE pellets are summarized in Table 1. As a general trend, all the physicochemical properties interesting for pyrolysis are within the ranges commonly established in literature for HDPE wastes [8,9].

Density has been calculated according to the ASTM D1895B Standard, whereas glass transition temperature and melting point have been determined by differential scanning calorimetry (DSC) in a Mettler Toledo DSC 822e apparatus according to the ASTM D3418 Standard. From the DSC analysis results, fusion enthalpy (ΔH_f) and latent heat of crystallization (ΔH_c) have been determined by integrating the area under each characteristic peak. The higher heating value (HHV) has been calculated using a Parr 369M 1356 Isoperibol Bomb calorimeter and the content of inorganic ash has been determined by calcination at 1000 °C in a Nabertherm LT 5/12 muffle furnace. The concentration of halogens (Cl, Br, P) has been determined by means of High Performance Liquid Chromatography/Ion Chromatography in a Dionex DX-100 ion chromatograph.

Table 1. Main physical properties of HDPE pellets.

Property	Value
Density (kg m^{-3})	957
HHV (MJ kg^{-1})	46.1
Inorganic ash (wt%)	0.99
DSC analysis	
Glass transition (°C)	118.5
Melting point (°C)	134.0
ΔH_f (kJ kg^{-1})	-204.8
ΔH_c (kJ kg^{-1})	206.3
Concentration of halogens (ppm)	
Chlorine	< 500*
Bromine	< 25*
Phosphorus	14.2

* below detection limit of the equipment

The compositional analysis of the HDPE pellets has been done by means of Fourier Transform Infrared Spectroscopy (FTIR) in a Shimadzu IRTracer-100 spectrometer

119 equipped with MIRacle 10 ATR sampling technique. Spectra have been collected in the
120 600-4000 cm^{-1} wave number range. The ATR-FTIR spectra of HDPE, both recycled and
121 pure, are shown in Figure 1, in which the identified absorbance bands all correspond to
122 C–H bond vibrations. Considering all the previous, it can be seen that both pure and
123 recycled HDPE have three main vibration bands (highlighted in grey in Figure 1) showing
124 the purity of the recycled HDPE. The vibration band located at ca. 500 cm^{-1} is assigned
125 to rocking vibrations of methylene groups (–CH_2–), that is, asymmetric flexion vibrations
126 caused by rotations within the plane, whereas at 1600–1480 cm^{-1} there is a C–H bending
127 band of CH_2 groups, meaning symmetric flexion vibrations in the plane [31]. Finally, the
128 vibrational bands located at 2875–2770 and 3000–2875 cm^{-1} are attributed to CH_2
129 symmetric and asymmetric stress-compression vibrations, respectively [32].
130 Additionally, an absorption band with weak intensity at 1025 cm^{-1} is observed in both
131 samples, connected to the wagging deformation of the CH_3 groups [33]. The absence of
132 vibrational bands above 3000 cm^{-1} and in the 1700–1470 cm^{-1} range suggests that the
133 sample presents a lineal and saturated nature.

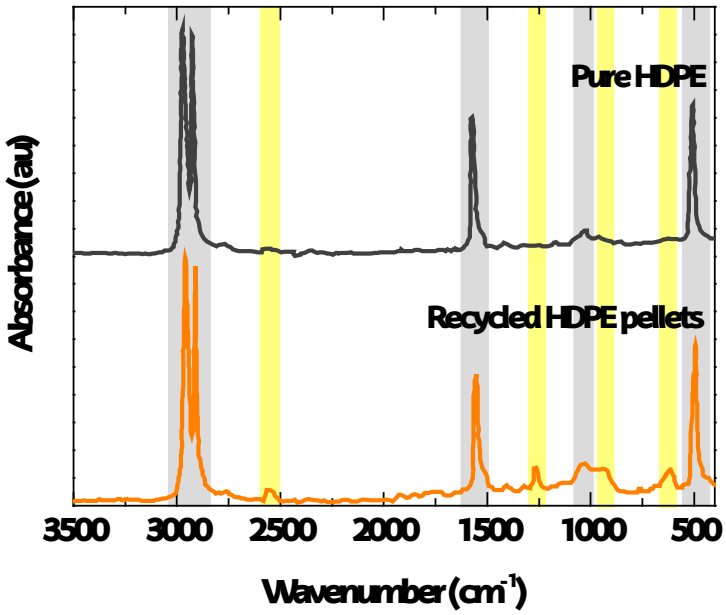

Figure 1. ATR-FTIR spectra of pure HDPE and recycled HDPE pellets.

It should be pointed out that four additional absorbance bands (highlighted in yellow in Figure 1) with weak intensity have been detected in the recycled pellets (at 2570, 1275, 960 and 625 cm^{-1}), which do not correspond neither with the composition of the HDPE nor with the bonds found in the pure sample. Thus, the presence of a possible polluting agent in the recycled HDPE pellets must be considered, possibly some kind of silicone trapped during mechanical recycling.

Thermal degradation analysis (results shown in Section 3.1) has been performed to determine the temperature range at which plastic degradation occurs and estimate its composition. The study has been carried out using a Mettler Toledo TGA2 Star^e System thermobalance in an inert N_2 atmosphere increasing temperature up to 600 °C at a 5 °C min^{-1} rate.

2.2. Reaction equipment and protocol

Slow thermal pyrolysis runs have been carried out in an AISI 316 stainless steel, high-pressure 1800 mL Parr batch autoclave (4570 Series) reactor, equipped with a heated oven, a thermocouple inside the vessel and a cooling coil, with maximum pressure and temperature capacities of 345 bar and 500 °C, respectively. Tested operating conditions have been: temperature, 430, 460 and 490 °C; and reaction time, 15–37.5–60 min. A typical experiment protocol is the following: the reactor is loaded with ca. 50 g of HDPE pellets and subsequently flushed with nitrogen to (i) expel air from the reactor ensuring the inertness of the reaction environment and (ii) perform a leak test (pressurizing up to 25 bar at room temperature and then returning to atmospheric pressure). Once absence of leaks is checked, at atmospheric pressure and with all the valves closed (discontinuous pyrolysis) the reactor is heated with an incremental rate of 15 ºC min^{-1} until the reaction temperature is reached and at this point zero time is established. The pressure of the reactor is continuously monitored. Once the reaction time has ended, a cooling coil located inside the reactor, which allows the circulation of water, cools down the reactor. After the run, gas products are collected in a gas-sampling bulb for their analysis by GC. The liquid PO product is separated from the remaining solids by vacuum filtration and dried until constant weight was attained at room temperature. Finally, PO is collected and stored on a refrigerated chamber to ensure its stability.

For each reaction run, the yields of oil and solids have been determined by weighing, whereas the gas production has been determined by mass difference of the starting weight of the charged reactor and the final weight of the depressurized reactor as follows:

$$\text{Yield of PO (wt\%)} = \frac{\text{mass of PO}}{\text{mass of HDPE}} \cdot 100 \quad (1)$$

$$\text{Yield of solids (wt\%)} = \frac{\text{mass of dried solids}}{\text{mass of HDPE}} \cdot 100 \quad (2)$$

$$\text{Yield of gas (wt\%)} = 100 - \text{Yield of PO} - \text{Yield of solids} \quad (3)$$

2.3. Product identification and analysis

Gas products are analysed through gas chromatography in an Agilent Technologies 6890 GC System equipped with: (i) a FID detector; (ii) a HP-PONA capillary column (length, 50 m; internal diameter, 0.20 mm; thickness, 0.50 μm); and, (iii) a CO_2 gas cylinder to reach cryogenic temperatures (-30 °C).

POs have been extensively analysed in order to determine their simulated distillation curve, composition of the naphtha and middle distillate fractions, and also their density and dynamic viscosity. Simulated distillation analyses have been carried out according to the ASTM D2887 Standard using an Agilent Technologies 6890 GC System, equipped with: (i) a FID detector; and (ii) a DB-2887 semi capillary column (length, 10 m; internal diameter, 0.53 mm; thickness, 3 μm). The composition of the naphtha fraction has been determined using the same GC setup as the one previously described for gas product analysis but without requiring cryogenic temperatures. Additionally, the compounds of the naphtha fraction have been identified according to the NIST 147 database by means of gas chromatography/mass spectrometry (GC-MS) analysis performed in a Shimadzu GC-MS QP2010S mass spectrometer coupled in line with a Shimadzu GC-2010 GC system. The composition of the middle distillates has been determined by means of comprehensive bi-dimensional gas chromatography (GC×GC) in an Agilent 7890 A chromatograph coupled to a mass spectrometer (MS) Agilent 5975C series GC/MSD provided with: (i) FID and MSD detectors; and (ii) a DB 5MS J&W 122–5532 (length,

30 m; internal diameter, 0.25 mm; thickness, 0.25 µm) and an HP-INNOWAX (length, 5 m; internal diameter, 0.25 mm; thickness, 0.15 µm) capillary columns connected by means of a valve-based flow modulator. The equipment has been previously described in detail elsewhere [34].

The density of PO has been measured according to the ASTM D6822 Standard, while dynamic viscosity tests have been carried out in a Brookfield DV-III ULTRA rheometer by using a thermal bath to maintain the temperature of the sample at 40.6 °C during the analysis.

3. Results

3.1. HDPE thermal degradation

As depicted in Figure 2, the degradation of the HDPE occurs over three different stages [35]. The first one takes place from 100 ºC to ca. 420 °C with a weight loss of 3 wt%, corresponding to the volatilization of low molecular weight species located in the smaller lateral chains that have suffered a scission via secondary radicals. The second stage, which starts at 420 ºC and ends at 500 °C, is associated with cracking reactions of the main hydrocarbon chains via primary radicals. Based on the derivative curve of the weight loss, it can be seen that the maximum weight loss rate is achieved at 479 °C. The last stage takes place above 500 °C as a consequence of the decomposition of the carbonaceous residue [36]. The obtained results are comparable to those reported in literature for virgin HDPE, proving the purity of the recycled HDPE pellets employed for the study [37,38].

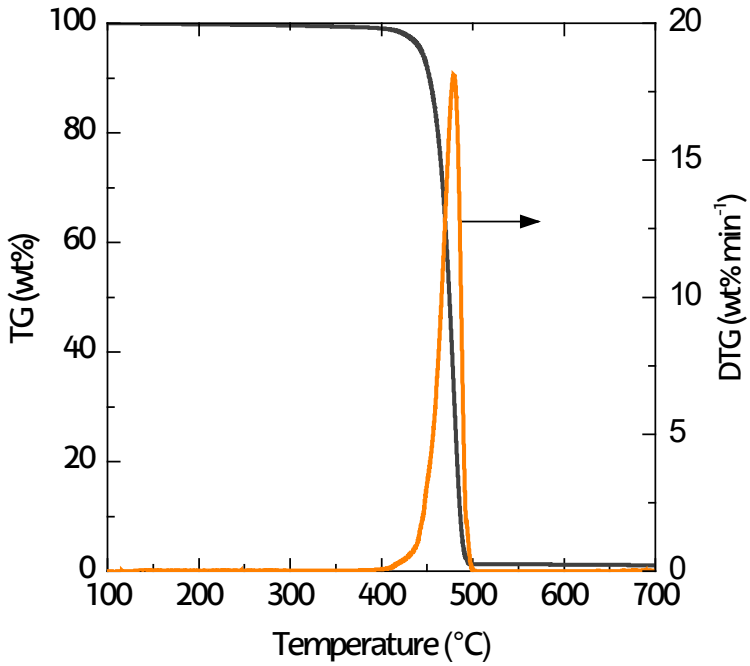

Figure 2. Non-isothermal TGA analysis of recycled HDPE pellets.

3.2. Product distribution in the slow pyrolysis of HDPE

The product yields obtained from the pyrolysis tests, namely gas, PO and solids, as well as the maximum pressures of each reaction run, are summarized in Table 2. Additionally, PO has been analyzed by means of simulated distillation analysis and classified into three different fractions based on a boiling point temperature (T_B) criteria: naphtha ($T_B < 216$ °C), middle distillates (MD) (216 °C < T_B < 343 °C) and heavy cycle oil (HCO) ($T_B > 343$ °C). From the obtained results (Table 2), we observed that both temperature and reaction time have a strong influence on product distribution. This way, upon increasing temperature and residence time the total pressure also increases, obtaining the highest gas product yield at the harshest operating conditions of 490 °C and 60 min, as a result of the enhancement of thermal cracking. Regarding their composition (Table S1), the main products on the gas phase are propane and propylene followed by ethane and ethylene, in agreement with literature [28,29]. The composition of the gases

231 makes them suitable for energy recovery in order to obtain the energy required for
232 pyrolysis. Besides, it is observed that reaction temperature has a relevant effect on the
233 composition of the gases. Thus, increasing the temperature increases the concentration of
234 paraffins and decreases that of olefins.

235 On the other hand, at higher temperatures and reaction times, a decrease in the PO yield
236 is observed, with a parallel increase in the yields of gases and solids. This result is due to
237 extent of propagation of homolytic cleavage process of simple C–C σ-type bonds and of
238 the propagation of subsequent radical chain reactions, which lead to the formation of
239 products with a lower molecular weight and hence increased tendency to vaporize [39].
240 However, at the same time, rates of secondary undesired reactions are also boosted
241 leading to the formation of higher amounts of solid products [10]. Then, considering the
242 obtained yields (Table 2), the optimal conditions should be those that maximize the
243 production of PO. This way, operating at a temperature of 430 °C, PO yields of 90.3–
244 80.1 wt% are obtained at all the investigated reaction time range. Additionally, working
245 at 460 °C an interesting PO yield of 79.9 wt% has been attained in a 15 min reaction.

246 **Table 2.** Product distribution and PO fractions at different operating conditions.

Temperature (°C)	Time (min)	Max. observed pressure (bar)	Product distribution (wt%)			PO fractions (wt%)		
			Gas	PO	Solid	Naphtha	MD	HCO
430	15	1	8.7	90.3	1.0	4.1	25.4	70.5
	37.5	5.50	14.2	84.8	1.0	34.4	34.9	30.7
	60	5.86	18.9	80.1	1.0	39.6	32.5	27.9
460	15	9.50	19.1	79.9	1.0	44.8	32.3	22.9
	37.5	15.75	38.8	59.5	1.7	64.6	26.6	8.8

	60	15.96	46.4	50.7	2.9	69.4	23.4	7.2
	15	20.90	59.3	37.4	3.3	72.2	20.6	7.2
490	37.5	18.93	60.6	34.5	4.9	75.2	18.1	6.7
	60	17.78	66.9	26.6	6.5	78.2	17.1	4.7

Focusing on the PO fractions (Table 2) and from the SD curves depicted in Figure 3, it can be seen that the pyrolysis temperature has a leading effect on the PO fraction distribution, while reaction time is secondary. This way, an increase in temperature from 430 to 490 °C implied a rise of the PO naphtha fraction at 15 min from 4.1 to 72.2 wt%. On the other hand, for a temperature of 460 °C, an increase of the reaction time from 15 to 60 min caused an increase of the naphtha fraction from 44.8 to 69.4 wt%, indicating that increasing the residence time enhances thermal cracking [29]. A similar tendency was observed by Das and Tiwari [40] studying the light (C_6–C_{11}) and middle (C_{12}–C_{20}) fractions of the PO obtained through low-temperature (300–400 °C) slow pyrolysis of virgin HDPE.

In order to obtain a proper idea of the suitability of the produced POs as a potential refinery stream, the simulated distillation curves of VGO and LCO (two conventional refinery streams) supplied by Petronor Refinery (Muskiz, Spain), have been included in the results shown in Figure 3 (VGO in Figure 3a and LCO in Figure 3c). It can be seen that all the POs are lighter than VGO. Just the PO obtained at 430 °C for a reaction time of 15 min (Figure 3a) has a similar distillation curve to that of the VGO, but more heterogeneous. On the other hand, the POs obtained at 430 and 460 °C (Figure 3b) show a distillation curve similar to that of the LCO with a lower initial boiling point and a higher final boiling point, having therefore a wider distribution of products. The POs obtained at 490 °C (Figure 3c) have distillation curves clearly lighter than that of the LCO, proving that thermal cracking reactions are highly boosted at this temperature.

Based on the aforementioned results, as the POs show a final boiling point lower than 500 °C, they can be considered as valuable feedstock for catalytic cracking or hydrocracking units combined with their current feedstock, i.e. VGO or LCO, respectively [41]. Indeed, this strategy has sound industrial prospects with a view to meeting the requirements for alternative feedstock in refineries. Therefore, as PO should be subjected to a subsequent upgrading stage in a refinery unit, an ideal PO should not be excessively light in order to minimize the gas production in the following stage. Hence, a PO with a moderate fraction of naphtha and high concentration of middle distillates would have the optimal composition. On the basis of the results in Table 2 and Figure 3 and considering the similarity of the distillation curves, the PO obtained at 430 °C and 15 min, with a content of naphtha, middle distillates and HCO of 4.1, 25.4 and 70.5 wt%, respectively, is appropriate for being co-fed together with VGO to the FCC unit. On the other hand, the POs obtained at 430 °C for reaction times of 37.5 and 60 min and at 460 °C for a reaction time of 15 min, with contents of naphtha, middle distillates and HCO of 34.4–44.8, 32.3–34.9 and 22.9–30.7 wt%, respectively, are suitable for being blended with LCO and fed to a hydroprocessing unit.

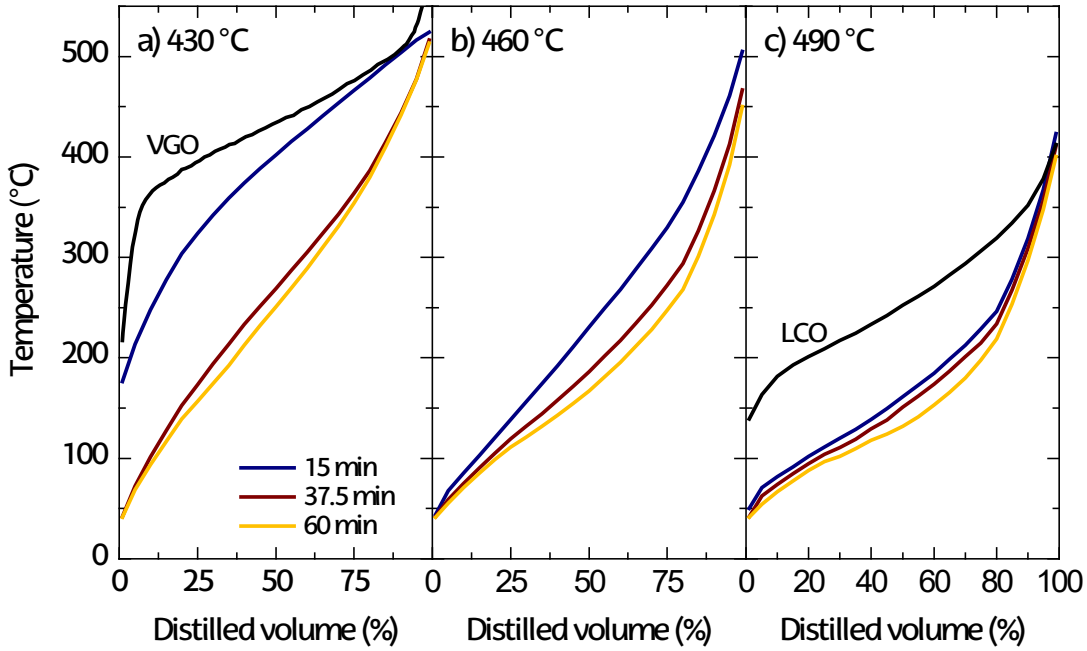

284

285 **Figure 3.** Simulated distillation curves for the different POs obtained at 430 °C (a),
286 460 °C (b) and 490 °C (c) at different reaction times.

287 Faussone [42] has assessed an industrial pyrolysis plant located in South East Asia that
288 synthesizes transportation fuel from waste feedstock. In the pyrolysis stage, they obtain a
289 liquid yield of ca. 65 wt% with a distribution of 40 wt% of naphtha, 45 %wt of LCO and
290 the remaining 15 wt% of HCO. These results are in concordance with those previously
291 designated in this section as the optimal ones, i.e. the liquid products obtained at 430 °C
292 for reactions of 37.5 and 60 min and the liquid product obtained at 460 °C for a reaction
293 time of 15 min (Table 2). Indeed, in our work, higher PO yields have been obtained (79.9–
294 84.8 wt%) under the same conditions, rendering the possible step-up in scale and size
295 encouraging.

296 *3.3. Composition of the PO fractions*

297 Due to the high content of naphtha and middle distillates of the POs, an analysis of each
298 fraction of the POs obtained at the different operating conditions has been performed by

299 gas chromatography. The main aim of these analyses is to determine the concentration of
300 the different hydrocarbon groups and assess the interest of each of these fractions
301 (naphtha, middle distillates …), which can be easily separated by distillation, for their
302 integration into the gasoline and diesel refinery pools.

303 *3.3.1. Naphtha*

304 The compounds of the naphtha fraction of the PO have been grouped according to their
305 chemical nature in: n-paraffins and iso-paraffins (P+iP), olefins (O) and aromatics (A) as
306 it can be seen in Figure 4. The hydrocarbon composition is strongly
307 temperature-dependent being at 430 °C (Figure 4a) is mainly dominated by paraffins and
308 olefins (44.0–73.7 and 22.3–43.1 wt%, respectively) with minor amounts of aromatics
309 (3.9–17.1 wt%). However, at 490 °C (Figure 4c) the naphtha fraction of the PO is
310 predominantly aromatic (51.6–72.2 wt%) with a lesser content of paraffins (9.6–
311 16.2 wt%).

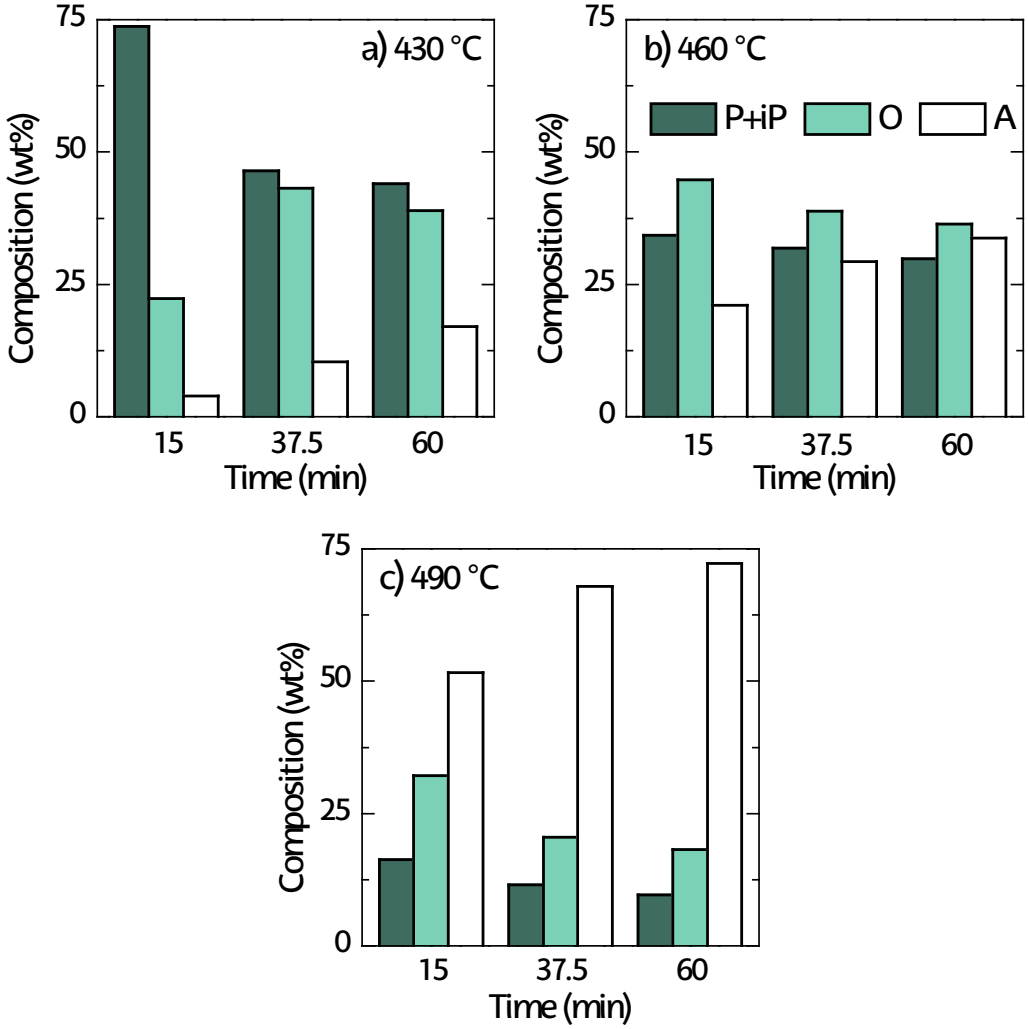

312

313 **Figure 4.** Composition of the naphtha fraction of the POs obtained at 430 °C (a), 460 °C
314 (b) and 490 °C (c) at different reaction times.

315 Paraffins are obtained through a free-radical transfer reaction in which an H atom bonded
316 to a C atom of a neighbor macromolecule of the polymer chain is extracted, leading to
317 the formation of a terminal methyl group (CH_3–R) and, consequently, propagating its
318 radical character [43]. This way, the reduction of the concentration of paraffins in the
319 naphtha fraction of the PO when both temperature and reaction time are increased is
320 consequence of the propagation of β-scission reactions, which lead to the formation of
321 olefins and diolefins as obtained molecules have at least one terminal vinyl group
322 (CH_2=CH–R) [22]. It should be specified that n-paraffins and iso-paraffins have been

323 grouped together for analysis of the data in Figure 4, given that the concentration of
324 iso-paraffins is negligible. This phenomenon occurs as the formation of iso-paraffins is
325 stereochemically and thermodynamically not favored due to the transpositions of the
326 methyl groups (CH_3–) [44].

327 A maximum olefin concentration is attained at the intermediate temperature of 460 °C
328 (Figure 4b) due to the increase of the β-scission type reactions. These reactions are
329 thermodynamically favored at higher temperatures as they require high amounts of
330 energy to break the adjacent C–C bond leading to the formation of smaller and
331 thermodynamically more unstable reaction intermediates [45]. A similar trend is observed
332 at longer reaction times; rather, the concentration of olefins goes through a maximum at
333 460 °C.

334 Furthermore, aromatics are obtained from the thermal cracking of long lineal polymeric
335 chains involving different reaction mechanisms: cyclization of olefins, condensation of
336 olefins and cyclization of n-paraffins. Through these reaction mechanisms a molecule of
337 naphthene is obtained, which is subsequently easily dehydrogenated into an aromatic
338 molecule due to the stability of the aromatic ring. Among the different aforementioned
339 reaction mechanisms, the most thermodynamically favored are cyclization and
340 condensation of olefins, being successive reactions to the β-scission that forms the olefins
341 from the polymer chains [46]. Therefore, this explains why aromatics increased both with
342 the reaction time and temperature in Figure 4, decreasing the olefin content.

343 The naphtha fraction has also been characterized on a carbon number basis and according
344 to the chemical structure of its components as shown in Figures S1-S3 in the
345 Supplementary Material, in which the evolution of the distribution of each group with the
346 reaction temperature and time is depicted. In the case of paraffins (Figure S1), at higher

347 temperatures cracking reactions are boosted leading to the formation of a higher amount
348 of lower molecular weight paraffins. Olefins (Figure S2) follow a similar trend than that
349 of the paraffins. When temperature is increased, olefins of lower molecular weight (C_5–
350 C_8) are produced because of the stabilization of β-scission reactions leading to a reduction
351 in the amount of long chain olefins (C_{10} and $C_{11\text{-}12}$). Finally, with regard to aromatics
352 (Figure S3), an increase in the reaction time and temperature favors the production of
353 alkyl-substituted aromatics. While the concentration of aromatics increases, dealkylation
354 reactions become more relevant leading to the formation of BTX fraction (benzene,
355 toluene, xylenes), which corresponds to C_6–C_8 molecules, respectively, and the reduction
356 of long chain alkyl aromatics (C_{10} and $C_{11\text{-}12}$). However, this latter reduction is not so
357 evident at 490 °C (Figure S3c), when condensation reactions are also boosted producing
358 naphthalene-type molecules, known to be coke precursors for their higher C/H ratio.

359 *3.3.2. Middle distillates*

360 The compositional analysis of the middle distillates fraction of the produced POs has been
361 carried out in an analogue way to the naphtha fraction in the previous section. As depicted
362 in Figure 5, a highly complex composition has been observed for middle distillates in
363 contrast to the naphtha fraction (Figure 4) and, hence, a more detailed compound
364 classification has been established, as follows: n-paraffins (nP), iso-paraffins (iP), olefins
365 (O), naphthenes (N), 1-ring aromatics (A_1), 2-ring aromatics (A_2) and 2^+-ring aromatics
366 (A_{2+}).

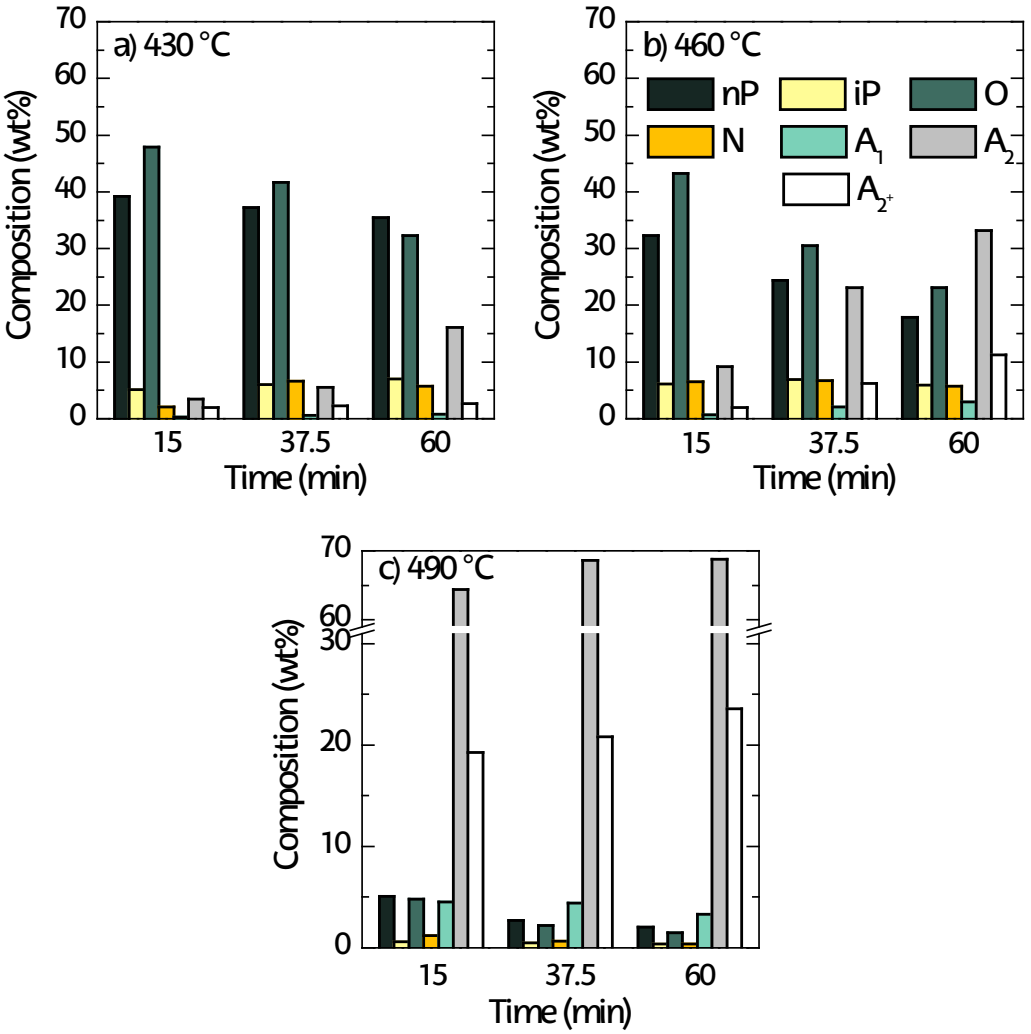

367

368 **Figure 5.** Composition of the MD fraction of PO obtained at 430 °C (a), 460 °C (b) and
369 490 °C (c) at different reaction times.

370 The strong impact of reaction temperature is again highlighted in the composition of the
371 MD fraction. This way, at 430 °C (Figure 5a) n-paraffins and olefins are the main
372 chemical groups with concentrations of 35.4–39.2 and 47.9–32.3 wt%, respectively, for
373 the different reaction times. It should be mentioned that the formation of 2-ring aromatics
374 is boosted at the highest reaction time as they increase from 3.5–5.6 to 16.1 wt%.
375 Typically, in pyrolysis the H/C atomic ratio decreases with temperature and reaction time,
376 which is consistent with the reported increasing aromaticity. Hence, the highest reaction
377 time (60 min) produces a decline in the H/C ratio favoring the aromatization processes

and the formation of small aromatic clusters that can be found both in liquid and solid products [47]. Focusing on the results obtained at 460 °C (Figure 5b), n-paraffins and olefins are still the main compounds, 32.3–17.8 and 43.3–23.1 wt%, respectively, although the concentration of 2 –ring aromatics starts to increase, particularly at reaction times higher than 15 min. This way, at 460 °C condensation and aromatization reactions become relevant in the reaction medium. On the other hand, at 490 ºC (Figure 5c) middle distillates show a significant aromatic nature, as these compounds account up to 95.7 wt% for the longest reaction time (60 min), with an important contribution of 2^{+}-ring aromatics (23.6 wt%). This aromatic formation occurs in pyrolysis processes at high temperature because of the breakage of polymer macromolecules into smaller fragments in the form of unstable molecules. Afterwards, these fragments recombine via pyro-synthesis, i.e. polymerization and aromatization reactions, to form more stable, larger molecules, e.g. aromatic compounds [48].

3.4. Comparison of the PO fractions with commercial fuels

The physicochemical properties of the POs obtained at the optimal conditions (430 °C and 37.5 min; 430 °C and 60 min; and, 460 °C and 15 min) have been measured and compared with those of commercial gasoline and diesel (Table 3). The obtained POs show an initial boiling point (IBP) of ca. 40 °C and a final boiling point (FBP) of ca. 510 °C. Regulations and specifications of automotive fuels set the boiling range for gasoline in 50–210 °C and for diesel in 172–350 °C according to Directive 98/70/EC of the European Parliament. Therefore, and in order for the boiling points of the naphtha and middle distillates fractions to fit in the ranges of gasoline and diesel, a reduction of the average molecular weight of the PO is required in order to comply with current legislation. For this purpose, POs must be subjected to an upgrading stage, e.g. catalytic

cracking or hydrotreating, as it has been previously laid out in Section 3.3, in order to reduce the amount of heavy molecules and increase the percentage of shorter chains C_5-C_{12} and/or C_{12}-C_{20}, which correspond to gasoline and diesel fuels, respectively.

Table 3. Comparison of the physical properties of the PO with those of the commercial gasoline and diesel and of the composition of the naphtha fraction with the specifications of the commercial fuels.

Property	PO	Gasoline	Diesel
Physical properties			
Density (kg m^{-3})[a]	789	720–778	957
HHV (MJ kg^{-1})[b]	45.4	42–46	42–45
IBP-FBP (°C)[c]	40–510	50–210	172–350
Chemical properties			
Sulfur content (ppm)	–	< 10	< 10
Olefins (wt%)	39–44*	< 18	–
Aromatics (wt%)	17–29*	< 35	–
Benzene (wt%)	–	< 1	–

Determined according to: [a] ASTM D6822 Standard; [b] ASTM D3523 Standard; [c] ASTM D2887 Standard.
* on the naphtha fraction

With regard to the restrictions in the chemical nature of commercial fuels, diesel has no specifications, whereas in the gasoline the content of olefins, aromatics and benzene is restricted. Thus, as naphtha fractions of the produced POs are mainly constituted of n-paraffins and olefins (31–44 and 39–44 wt%, respectively), their composition does not comply with the limits, as the concentration of olefins must be below 18 wt%. However, the concentration of aromatics (17–29 wt%) is lower than that established by the legislation. Consequently, the goal of reducing the content of olefins can be reached by means of a mild hydrotreatment stage in refinery, i.e. moderate pressure and temperature,

of the raw PO or of the PO naphtha fraction previously separated by distillation. On the other hand, sulfur restrictions are avoided for POs, as no sulfur has been detected in them. Therefore, after the mild hydrotreating stage, the PO or the naphtha of PO would have an appropriate composition to be blended with refinery streams with higher aromatic content, which is a really interesting strategy for the valorization of secondary refinery streams, such as LCO.

The average high heating value (HHV) for the POs has been higher than 45 MJ kg^{-1}, which can be assumed as suitable to be used as a source of energy being contained within the range of commercial gasoline (42–46 MJ kg^{-1}) and close to that of commercial diesel (42–45 MJ kg^{-1}). The density of the POs (798 kg m^{-3}), is located between the values established for gasoline and diesel. This indicates that after a proper distillation and separation of the fractions, their density would be the required.

4. Conclusions

The slow pyrolysis of recycled HDPE has proven to be a promising management technique in order to obtain a high yield of liquid product (PO) whose composition and properties are adequate to be integrated into conventional refinery streams, such as VGO or LCO. Afterwards, in the refinery, by means of cracking or hydrocracking, the composition of the PO will be tuned to comply with the requirements established for automotive fuels.

An increase in either the pyrolysis temperature and/or reaction time promotes the formation of gaseous products (C_1–C_5), producing gas yields up to 70 wt% operating at 490 °C. Consequently, pyrolysis should be carried at 430 °C and short reaction times (15 min) in order to maximize the production of PO (90.3 wt%). The simulated

distillation curve of this PO is similar to that of the vacuum gasoil (VGO), rendering it suitable to be co-fed with VGO to the fluidized catalytic cracking (FCC) unit.

The PO obtained at 430 °C at longer reaction times and 460 °C, is appropriate to be co-fed together with light cycle oil (LCO) to a hydroprocessing unit. This PO has high contents of naphtha and middle distillates, in the ranges of 34.4–69.4 and 23.4–34.9 wt% (depending on the reaction time), respectively. Thereby, the high content of olefins of the naphtha fraction, which can easily be separated by distillation, will require a mild hydrotreatment before its blending into the gasoline pool. Furthermore, the negligible content of sulfur and the low content of aromatics boost the interest of this PO for its valorization together with aromatic refinery streams, e.g. LCO.

Consequently, a combined strategy of slow pyrolysis of recycled HDPE plastic together with a subsequent catalytic cracking or hydroprocessing stage for the final production of fuels in refinery (waste refinery) offers promising results in an economically viable manner for the large-scale chemical recycling of plastic. The employment of already depreciated refinery units for the PO tuning reactions (hydrotreatment or cracking) and subsequent conditioning of the products as fuels is key for the economic viability of the initiative. In addition, through this strategy, the industrial implementation of the pyrolysis units would be facilitated, with the consequent thrust to the development of pyrolysis technologies and the recycling industry.

Acknowledgements

This work has been carried out with financial support of the Ministry of Science, Innovation and Universities (MICINN) of the Spanish Government (grant RTI2018-096981-B-I00), the Basque Government (grant IT2018-19), the European Union's ERDF

462 funds and the European Commission (HORIZON H2020-MSCA RISE-2018. Contract
463 No. 823745).

464 The authors also acknowledge Petronor Refinery for providing the LCO and VGO used
465 in this work.

466

467 **References**

468 [1] PEMRG Plastics Europe's Market Research and Statistics Group. Plastics the facts
469 2018. An analysis of European plastics production, demand and waste data.
470 Brussels: 2018.

471 [2] Heidbreder LM, Bablok I, Drews S, Menzel C. Tackling the plastic problem: A
472 review on perceptions, behaviors, and interventions. Sci Total Environ
473 2019;668:1077–93. doi:10.1016/j.scitotenv.2019.02.437.

474 [3] Chae Y, An Y-J. Current research trends on plastic pollution and ecological
475 impacts on the soil ecosystem: A review. Environ Pollut 2018;240:387–95.
476 doi:10.1016/j.envpol.2018.05.008.

477 [4] Haward M. Plastic pollution of the world's seas and oceans as a contemporary
478 challenge in ocean governance. Nat Commun 2018;9:667. doi:10.1038/s41467-
479 018-03104-3.

480 [5] Blettler MCM, Abrial E, Khan FR, Sivri N, Espinola LA. Freshwater plastic
481 pollution: Recognizing research biases and identifying knowledge gaps. Water Res
482 2018;143:416–24. doi:10.1016/j.watres.2018.06.015.

483 [6] Maris J, Bourdon S, Brossard J-M, Cauret L, Fontaine L, Montembault V.
484 Mechanical recycling: Compatibilization of mixed thermoplastic wastes. Polym
485 Degrad Stab 2018;147:245–66. doi:10.1016/j.polymdegradstab.2017.11.001.

486 [7] Al-Salem SM, Lettieri P, Baeyens J. Recycling and recovery routes of plastic solid
487 waste (PSW): A review. Waste Manag 2009;29:2625–43.
488 doi:10.1016/j.wasman.2009.06.004.

489 [8] Datta J, Kopczyńska P. From polymer waste to potential main industrial products:
490 Actual state of recycling and recovering. Crit Rev Environ Sci Technol

2016;46:905–46. doi:10.1080/10643389.2016.1180227.

[9] Al-Salem SM, Antelava A, Constantinou A, Manos G, Dutta A. A review on thermal and catalytic pyrolysis of plastic solid waste (PSW). J Environ Manage 2017;197:177–98. doi:10.1016/j.jenvman.2017.03.084.

[10] Lopez G, Artetxe M, Amutio M, Bilbao J, Olazar M. Thermochemical routes for the valorization of waste polyolefinic plastics to produce fuels and chemicals . A review. Renew Sustain Energy Rev 2017;73:346–68.

[11] Fivga A, Dimitriou I. Pyrolysis of plastic waste for production of heavy fuel substitute: A techno-economic assessment. Energy 2018;149:865–74. doi:10.1016/j.energy.2018.02.094.

[12] Lopez G, Artetxe M, Amutio M, Alvarez J, Bilbao J, Olazar M. Recent advances in the gasification of waste plastics. A critical overview. Renew Sustain Energy Rev 2018;82:576–96. doi:10.1016/j.rser.2017.09.032.

[13] Elordi G, Olazar M, Lopez G, Artetxe M, Bilbao J. Product yields and compositions in the continuous pyrolysis of high-density polyethylene in a conical spouted bed reactor. Ind Eng Chem Res 2011;50:6650–9. doi:10.1021/ie200186m.

[14] Aguado J, Serrano DP, Escola JM, Garagorri E. Catalytic conversion of low-density polyethylene using a continuous screw kiln reactor. Catal Today 2002;75:257–62. doi:10.1016/S0920-5861(02)00077-9.

[15] Marcilla A, Hernández M del R, García ÁN. Degradation of LDPE/VGO mixtures to fuels using a FCC equilibrium catalyst in a sand fluidized bed reactor. Appl Catal A Gen 2008;341:181–91. doi:10.1016/j.apcata.2008.02.041.

[16] Elordi G, Olazar M, Lopez G, Artetxe M, Bilbao J. Continuous polyolefin cracking on an HZSM-5 zeolite catalyst in a conical spouted bed reactor. Ind Eng Chem Res

515 2011;50:6061–70. doi:10.1021/ie2002999.

516 [17] Kassargy C, Awad S, Burnens G, Kahine K, Tazerout M. Gasoline and diesel-like
517 fuel production by continuous catalytic pyrolysis of waste polyethylene and
518 polypropylene mixtures over USY zeolite. Fuel 2018;224:764–73.
519 doi:10.1016/j.fuel.2018.03.113.

520 [18] Artetxe M, Lopez G, Amutio M, Elordi G, Bilbao J, Olazar M. Light olefins from
521 HDPE cracking in a two-step thermal and catalytic process. Chem Eng J
522 2012;207–208:27–34. doi:10.1016/j.cej.2012.06.105.

523 [19] Artetxe M, Lopez G, Amutio M, Elordi G, Bilbao J, Olazar M. Cracking of high
524 density polyethylene pyrolysis waxes on HZSM-5 catalysts of different acidity.
525 Ind Eng Chem Res 2013;52:10637–45. doi:10.1021/ie4014869.

526 [20] Arandes JM, Abajo I, López-Valerio D, Fernández I, Azkoiti MJ, Olazar M, et al.
527 Transformation of Several Plastic Wastes into Fuels by Catalytic Cracking. Ind
528 Eng Chem Res 1997;36:4523–9. doi:10.1021/ie970096e.

529 [21] Arandes JM, Ereña J, Azkoiti MJ, Olazar M, Bilbao J. Thermal recycling of
530 polystyrene and polystyrene-butadiene dissolved in a light cycle oil. J Anal Appl
531 Pyrolysis 2003;70:747–60. doi:10.1016/S0165-2370(03)00056-1.

532 [22] Odjo AO, García AN, Marcilla A. Conversion of low density polyethylene into
533 fuel through co-processing with vacuum gas oil in a fluid catalytic cracking riser
534 reactor. Fuel Process Technol 2013;113:130–40.
535 doi:10.1016/j.fuproc.2013.03.008.

536 [23] Biswas S, Sharma DK. Co-cracking of jatropha oil, vacuum residue and HDPE and
537 characterization of liquid, gaseous and char products obtained. J Anal Appl
538 Pyrolysis 2013;101:17–27. doi:10.1016/j.jaap.2013.03.003.

539 [24] Biswas S, Majhi S, Mohanty P, Pant KK, Sharma DK. Effect of different catalyst
540 on the co-cracking of Jatropha oil, vacuum residue and high density polyethylene.
541 Fuel 2014;133:96–105. doi:10.1016/j.fuel.2014.04.082.

542 [25] Palos R, Gutiérrez A, Arandes JM, Bilbao J. Upgrading of high-density
543 polyethylene and light cycle oil mixtures to fuels via hydroprocessing. Catal Today
544 2018;305:212–9. doi:10.1016/j.cattod.2017.06.033.

545 [26] Munir D, Irfan MF, Usman MR. Hydrocracking of virgin and waste plastics: A
546 detailed review. Renew Sustain Energy Rev 2018. doi:10.1016/j.rser.2018.03.034.

547 [27] Kohli K, Prajapati R, Maity SK, Sharma BK. Hydrocracking of heavy
548 crude/residues with waste plastic. J Anal Appl Pyrolysis 2019;140:179–87.
549 doi:10.1016/j.jaap.2019.03.013.

550 [28] Owusu PA, Banadda N, Zziwa A, Seay J, Kiggundu N. Reverse engineering of
551 plastic waste into useful fuel products. J Anal Appl Pyrolysis 2018;130:285–93.
552 doi:10.1016/j.jaap.2017.12.020.

553 [29] Kumari A, Kumar S. Pyrolytic degradation of polyethylene in autoclave under high
554 pressure to obtain fuel. J Anal Appl Pyrolysis 2017;124:298–302.
555 doi:10.1016/j.jaap.2017.01.020.

556 [30] Das P, Tiwari P. Valorization of packaging plastic waste by slow pyrolysis. Resour
557 Conserv Recycl 2018;128:69–77. doi:10.1016/j.resconrec.2017.09.025.

558 [31] da Silva DJ, Wiebeck H. Using PLS, iPLS and siPLS linear regressions to
559 determine the composition of LDPE/HDPE blends: A comparison between
560 confocal Raman and ATR-FTIR spectroscopies. Vib Spectrosc 2017;92:259–66.
561 doi:10.1016/j.vibspec.2017.08.009.

562 [32] Sadighzadeh A, Azimzadeh Asiabi P, Ramazani A, Ghoranneviss M, Salar Elahi

563 A. Characterization of gamma irradiated low and high density polyethylene using
564 the FTIR and DSC technique. J Inorg Organomet Polym Mater 2015;25:1448–55.
565 doi:10.1007/s10904-015-0258-6.

566 [33] Babaghayou MI, Mourad A-HI, Lorenzo V, de la Orden MU, Martínez Urreaga J,
567 Chabira SF, et al. Photodegradation characterization and heterogeneity evaluation
568 of the exposed and unexposed faces of stabilized and unstabilized LDPE films.
569 Mater Des 2016;111:279–90. doi:10.1016/j.matdes.2016.08.065.

570 [34] Palos R, Gutiérrez A, Arandes JM, Bilbao J. Catalyst used in fluid catalytic
571 cracking (FCC) unit as a support of NiMoP catalyst for light cycle oil
572 hydroprocessing. Fuel 2018;216:142–52. doi:10.1016/j.fuel.2017.11.148.

573 [35] Cuadri AA, Martín-Alfonso JE. The effect of thermal and thermo-oxidative
574 degradation conditions on rheological, chemical and thermal properties of HDPE.
575 Polym Degrad Stab 2017;141:11–8. doi:10.1016/j.polymdegradstab.2017.05.005.

576 [36] Baena L, Zuleta E, Calderón J. Evaluation of the stability of polymeric materials
577 exposed to palm biodiesel and biodiesel–organic acid blends. Polymers (Basel)
578 2018;10:511. doi:10.3390/polym10050511.

579 [37] Fávaro SL, Rubira AF, Muniz EC, Radovanovic E. Surface modification of HDPE,
580 PP, and PET films with KMnO4/HCl solutions. Polym Degrad Stab
581 2007;92:1219–26. doi:10.1016/j.polymdegradstab.2007.04.005.

582 [38] Kumar S, Singh RK. Thermolysis of high-density polyethylene to petroleum
583 products. J Pet Eng 2013;2013:1–7. doi: 10.1155/2013/987568

584 [39] Amini E, Safdari M-S, DeYoung JT, Weise DR, Fletcher TH. Characterization of
585 pyrolysis products from slow pyrolysis of live and dead vegetation native to the
586 southern United States. Fuel 2019;235:1475–91. doi:10.1016/j.fuel.2018.08.112.

587 [40] Das P, Tiwari P. The effect of slow pyrolysis on the conversion of packaging waste
588 plastics (PE and PP) into fuel. Waste Manag 2018;79:615–24.
589 doi:10.1016/j.wasman.2018.08.021.

590 [41] Arabiourrutia M, Elordi G, Lopez G, Borsella E, Bilbao J, Olazar M.
591 Characterization of the waxes obtained by the pyrolysis of polyolefin plastics in a
592 conical spouted bed reactor. J Anal Appl Pyrolysis 2012;94:230–7.
593 doi:10.1016/j.jaap.2011.12.012.

594 [42] Faussone GC. Transportation fuel from plastic: Two cases of study. Waste Manag
595 2018;73:416–23. doi:10.1016/j.wasman.2017.11.027.

596 [43] Poutsma ML. The radical stabilization energy of a substituted carbon-centered free
597 radical depends on both the functionality of the substituent and the ordinality of
598 the radical. J Org Chem 2011;76:270–6. doi:10.1021/jo102097n.

599 [44] Christensen ED, Chupka GM, Luecke J, Smurthwaite T, Alleman TL, Iisa K, et al.
600 Analysis of oxygenated compounds in hydrotreated biomass fast pyrolysis oil
601 distillate fractions. Energy Fuels 2011;25:5462–71. doi:10.1021/ef201357h.

602 [45] Zhai Y, Ao C, Feng B, Meng Q, Zhang Y, Mei B, et al. Experimental and kinetic
603 modeling investigation on methyl decanoate pyrolysis at low and atmospheric
604 pressures. Fuel 2018;232:333–40. doi:10.1016/j.fuel.2018.05.145.

605 [46] Müller S, Liu Y, Vishnuvarthan M, Sun X, van Veen AC, Haller GL, et al. Coke
606 formation and deactivation pathways on H-ZSM-5 in the conversion of methanol
607 to olefins. J Catal 2015;325:48–59. doi:10.1016/j.jcat.2015.02.013.

608 [47] Janković B, Manić N, Dodevski V, Popović J, Rusmirović JD, Tošić M.
609 Characterization analysis of Poplar fluff pyrolysis products. Multi-component
610 kinetic study. Fuel 2019;238:111–28. doi:10.1016/j.fuel.2018.10.064.

611 [48] Ly HV, Choi JH, Woo HC, Kim S-S, Kim J. Upgrading bio-oil by catalytic fast
612 pyrolysis of acid-washed Saccharina japonica alga in a fluidized-bed reactor.
613 Renew Energy 2019;133:11–22. doi:10.1016/j.renene.2018.09.103.